INTERNATIONAL JOURNAL OF INTEGRATED ENGINEERING
ISSN: 2229-838X e-ISSN: 2600-7916

IJIE

Vol. 17 No. 4 (2025) 42-54
https://publisher.uthm.edu.my/ojs/index.php/ijie

An Experimental Evaluation of the Effects of Relative Draft and Centre of Gravity Position on the Performance Wave Energy Converter

Noh Zainal Abidin[1]*, Mohd Rashdan Saad[2], Mohd Rosdzimin Abdul Rahman[2], Mohd Norsyarizad Razali[1], Ameer Suhel[2], Mohamad Azrin Abd Azis[1], Mohd Najib Abdul Ghani Yolhamid[1], Zulkifly Mat Radzi[1]

[1] *Faculty of Defence and Science Technology,*
Universiti Pertahanan Nasional Malaysia, Kem Sungai Besi 57000, Kuala Lumpur, MALAYSIA
[2] *Faculty of Engineering,*
Universiti Pertahanan Nasional Malaysia, Kem Sungai Besi 57000 Kuala Lumpur, MALAYSIA

*Corresponding Author: noh@upnm.edu.my
DOI: https://doi.org/10.30880/ijie.2025.17.04.004

Article Info

Received: 10 September 2024
Accepted: 28 December 2024
Available online: 30 August 2025

Keywords

Wave energy converter, primary conversion efficiency, FOWC, BBDB, optimization, flume wave tank, draft, hydrodynamic performance, COG

Abstract

Prior studies highlight that the Backward Bent Duct Buoy (BBDB) is one of the simplest and most robust wave energy converters (WECs). However, the impact of relative draft and the location of the center of gravity (COG) on the hydrodynamic performance of the BBDB remains inconsistent and underexplored in the field. Thus, this study investigates the optimal relative draft and center of gravity (COG) location for maximizing the hydrodynamic performance of the Backward Bent Duct Buoy (BBDB), a simple and robust wave energy converter. The research explores the influence of different drafts and COG locations across wave heights (0.03 m, 0.04 m, 0.05 m) and periods (1s to 2s) using the OMEY's flume wave tank. A Froude scale of 1:13 was applied to the BBDB model. Verification and validation with previous studies yielded a percentage difference of 0.22%. Results show that a draft of T=0.3m (T/D=0.53) with an upright COG achieves the highest conversion efficiency of 56.7% at a wave height of 0.05 m, outperforming other configurations. Lower efficiency of 16.1% was noted for the Port COG at H=0.03m. The T=0.3m draft with the exact COG maximizes heave and pitch oscillations, enhancing internal air pressure variations and overall energy conversion. Appropriate COG positioning and draft are key to achieving resonance, reducing drag, and improving performance. This study emphasizes the significance of draft and COG location in optimizing BBDB design and operation, particularly in low wave height conditions.

1. Introduction

Since the oceans comprise 70% of the Earth's surface and wave at an average power of 2.1 TW, research on the Wave Energy Converter (WEC) is concentrated there [1]. Wave energy represents a largely untapped renewable resource, with the potential to provide substantial power generation to coastal regions, which is particularly crucial given the increasing demand for clean energy sources. Hence, compared to solar and wind energy sources, which can only create about 25% of the energy needed, the ocean has the capacity to produce up to 90% more energy [2]. However, despite its potential, wave energy remains underutilized due to technological challenges and limitations in conversion efficiency, reliability, and device optimization. The use of renewable energy sources, like

wind, sun, and ocean waves, is growing as a result of the depletion of fossil fuel reserves and the acceleration of global warming [3]. A great deal of research has been done to find alternatives to fossil fuels, which are running out and emit toxic pollutants that are bad for human health [4].

In this context, the development of effective WEC technologies like the Backward Bent Duct Buoy (BBDB) is critical. The BBDB, designed for large-wave power extraction, offers a promising solution due to its robust and simple design. In order to capture wave energy and transform it into electrical power, Babarit divides WEC into three primary categories: oscillating water columns (OWC), wave-activated bodies (WAB), and overtopping devices (OD) [5]. The OWC, a popular coastal wave energy device, is frequently placed on or near cliffs or rocky outcrops that are adjacent to the deep-sea floor. They are made up of a cavity that is connected to the beach and partially submerged, which transforms wave energy into air pressure [6]. According to Amarasekara and Jebli & Chagdali stated that the OWC is the most promising WEC since it is robust, useful in near-shore locations, and capable of capturing energy from low-energy seas [3],[7]. OWC technology has also been successfully applied in a number of power plants, including the 500kW LIMPET [8], the OE buoy [9], the 100 kW Shanwei OWC [10], and others. Despite these successes, existing WECs, including OWCs and BBDBs, face challenges in terms of optimizing design for varying wave conditions and improving energy conversion efficiency. The OWC technologies have shown promise and will benefit from more study and advancement in the future.

According to Badhurshah, there are three steps involved in the OWC operating principle. First, compressed air is created in a vertical column using the water level [11]. The compressed air then goes through a conversion stage where a turbine is used to convert it into mechanical energy. Ultimately, a generator is used to transform this mechanical energy into electrical power. There are two types of OWC systems: floating OWC systems and fixed OWC systems. These devices usually work in a similar way, using the air in the air chamber to move back and forth and towards the air turbine at the top of the device to generate energy. An electrical generator is then linked to this turbine. One key challenge in WEC development is optimizing device geometry and positioning to maximize energy capture across different sea states, which remains a critical research gap in advancing the technology.

Compared to a fixed system, the main advantage of an OWC-type floating system is its ability to capture ocean wave energy both close and far from the coast. However, the fixed OWC can only extract the wave energy in close proximity to the beach. Wu's study indicates that the WAB and OD devices are not as efficient at converting energy as the floating OWC. Its floating construction, which consists of a single shell structure and is both economical and simple, is the cause of its simplicity. Additionally, optimizing the relative draft and center of gravity (COG) positioning of floating devices like the BBDB is essential for enhancing hydrodynamic performance and stability, yet these aspects remain underexplored in current literature. The first version of Yoshio Masuda's floating Oscillating Water Column (OWC) gadget, a navigation buoy driven by wave energy, was created in the 1940s.

Yoshio Masuda is recognized by Falcão & Henriques as the creator of modern wave energy technology, which uses a unidirectional air turbine together with rectifying valves in a power take-off (PTO) system to power navigation buoys [8]. Large-scale WEC Kaimei was developed in the 1980s, building upon its predecessor. However, due to insufficient effectiveness, Yoshio Masuda and his group decided to remodel the floating OWC concept. They chose the BBDB model, which is an L-shaped OWC with its back facing the waves. This specific OWC can be placed simply near the shoreline and does not require a large depth of water. Further research is needed to understand how modifications in BBDB design—such as changes in draft and COG—can enhance its performance under different wave conditions, which is critical for the deployment of efficient WEC systems in diverse marine environments.

It was reported by [8],[12] and [13] that the BBDB was created for large-wave power and the most successful OWC. The BBDB design provides reduced anchoring force and cost, shorter floating structures, and higher conversion efficiency when compared to other floating OWCs. A 1:4 scale BBDB prototype with an axial flow self-rectifying impulse turbine and Wells turbines was tested in Ireland in 2008. Previous research has shown that the geometrical shapes of BBDB that influence hydrodynamic performance are corner, buoy, and extension duct length. Enhancing hydrodynamic performance requires an understanding of the lifting and drag forces that arise from the water-solid interaction. Despite previous efforts, there is still a need to address the limitations related to the influence of draft and COG on the BBDB's energy extraction efficiency, especially in varying sea states. Hydrodynamic performance towards submerged bodies, such as hydrofoils, is influenced by lift and drag [14]. The air chamber of BBDB needs to be large for maximum efficiency in order to prevent water ingestion from the air turbine [13]. The maximum efficiency of WEC has been validated by multiple OWC chamber sizing studies [8]. Toyota et al. (2009) reported that the efficiency of BBDB was enhanced by multiple geometrical optimizations [15]. The current study aims to fill this gap by examining the effects of various drafts and COG positions on BBDB efficiency, focusing on optimizing its design for enhanced hydrodynamic performance and energy conversion.

Ashlin et. al [16] explored combining a BBDB with an oscillating water column, creating a multifunctional floating structure that reduces wave-generated losses. The addition of a BBDB component stabilized the system by moderating vertical movement, inspiring further studies on corner shape optimization for better efficiency.

Int. Journal of Integrated Engineering Vol. 17 No. 4 (2025) p. 42-54

Earlier research has focused mainly on BBDB geometry to improve primary conversion efficiency. Abidin et al. expanded this by analyzing the impact of BBDB heading angles on performance in the OMEY flume wave tank, highlighting stability and safety issues per IMO standards [20]. Their study revealed that stern wave conditions (0°) offered the highest efficiency (45.6%), while head waves (180°) were the least effective. These findings underscore the adaptive potential of BBDB in varied sea conditions [21]. Building on these studies, this research examines how different drafts and COG positions affect BBDB efficiency. A suitable draft ensures responsive buoy motions, optimizing pitch and heave while reducing drag. Proper COG positioning influences natural frequencies of these motions, enhancing resonance and energy extraction [23]. Froude scaling (1:13) was employed to maintain dynamic similarity between the model and full-scale BBDB. This approach ensures that wave interactions, hydrodynamic forces, and energy conversion processes observed in the model are representative of full-scale conditions. The scaled wave conditions of 0.03m to 0.05m heights correspond to full-scale wave heights of 0.39m to 0.65m, reflecting typical wave conditions in Malaysian waters. This scaling allows for accurate extrapolation of model data to real-world scenarios in future.

Nomenclature	
L	length, m
h	depth, m
B	width, m
A_i	amplitude of incident wave, m
H	significance Wave Height, m
T	wave Period, s
M	mass, kg
E_{air}	energy airflow, kW
E_{wave}	energy of an incident wave, kW
C_g	group velocity, m/s
$Q(t)$	the airflow rate through the PTO,m^3/s
$\Delta P(t)$	chamber differential air pressure, Pa
k	wave number
g	acceleration of gravity (m/s^2)
Greek symbols	
η	primary conversion efficiency/capture width ratio
λ	wave length,m
Abbreviations	
BBDB	backward bent duct bouy
PTO	power take off
PLA	polylactic acid
CAD	computer aided design
AP	aft perpendicular (rear BBDB)
FP	forward perpendicular (front BBDB)

2. Experimental Setup

This research utilized the BBDB model and orifice had formed by using Flash Forged 3D Printer with Polylactic Acid (PLA) filament material based on Abidin et al (2024). [20]. The BBDB type round bottom corner with Acrylic material was utilized in this research as shown in Fig. 1 based on Jalani et al. (2022) [19]. The particulars of BBDB is shown in Table 1.

Table 1 *BBDB model particulars [2]*

Description	Symbol / unit	Model (1:13)
Length Overall,	L (m)	0.91
Breadth	B (m)	0.6
Depth (deck)	D (m)	0.565
Depth (Inlet chamber)	D_b (m)	0.195
Draft	T (m)	0.35
Weight	m (kg)	65.37
Longitudinal Centre Gravity	LCG (m)	0.455
Vertical Centre Gravity	VCG (m)	0.2825
Tranverse Centre Gravity	TCG (m)	0

As mentioned earlier, the experiment was conducted in heading angle stern wave (0°) which obtained the highest efficiency as referred in Abidin et al. (2024) [20]. By utilizing the parameter in Table 1, the research was conducted on four different drafts at T= 0.3m, 0.33m, 0.35m and 4m to inspect the influence towards efficiency obtained. The ship terminology for BBDB as in Fig. 2 [21].

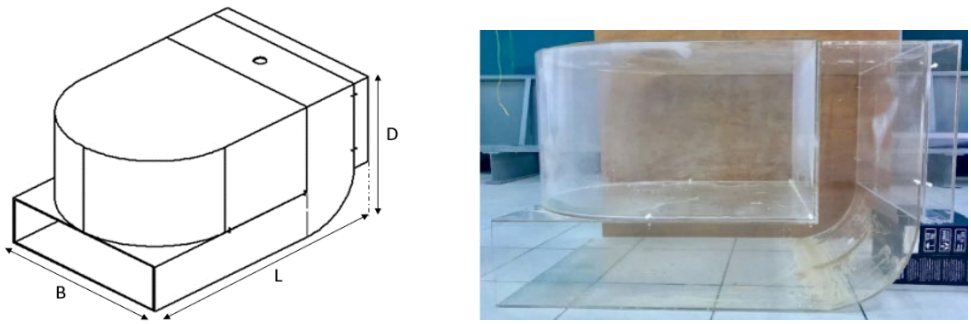

Fig. 1 *Isometric and side view of BBDB model [17]*

The buoyancy of the BBDB is depending on the fore and rear bouy (green) to give sufficiently buoyancy force. Fig. 2 illustrates the inlet/outlet ducting of BBDB. The draft and COG required can be setup based on the additional load arrangement to be placed inside the front bouy. Generally, the exact mass for BBDB was 24.47kg, However, in order to get the BBDB in the upright position with 0^0 trim and heel, the additional load, m=37.7kg placed in the centre front bouy (blue) to ensure the LCG, VCG and TCG, draft required achieved as in Table 1.

Int. Journal of Integrated Engineering Vol. 17 No. 4 (2025) p. 42-54

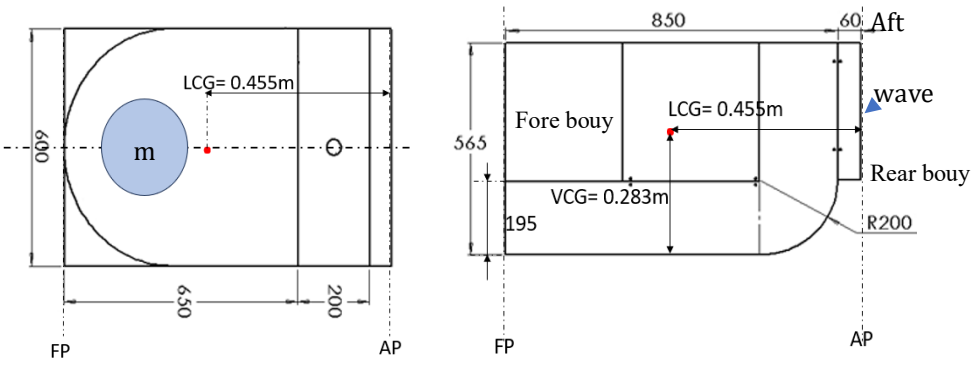

Fig. 2 *BBDB terminology for stern wave position (a) Top view; (b) Side view*

The study begins by referencing prior research which demonstrates the optimal operation of the BBDB. The geometric selection, specifically a round bottom corner, follows the guidelines from Jalani et al. (2022) [19]. For the BBDB's wave heading angle, the stern wave heading angle is employed based on the recommendations from Abidin et al. (2024) [20]. To measure water levels and wave elevation within the flume tank, three KEYENCE FW-H07 digital ultrasonic water level sensors with an accuracy of 0.001 m are utilized. The flow rate at the orifice is measured using an EXTECH HD-350 pitot tube anemometer, with a precision of 0.0001 m^3/min, and a KEYENCE AP-10S air pressure sensor with an accuracy of 0.01 kPa. All sensors are integrated with the KEYENCE NR-500 Data Acquisition System (DAQ) connected to workstations, as depicted in Fig. 3. An elbow connection, fabricated for the experiment, is installed on top of the orifice and sealed with silicone to prevent air leakage. The BBDB is anchored to the bottom of the wave tank using four lines of rope, securing it on both the left and right sides. This setup allows the BBDB to free float, enhancing its heave and pitch motions, which is expected to improve energy production efficiency as indicated by Gadelho et al. (2021)[18]. After all sensors are connected to the BBDB, readings are monitored through the KEYENCE Wavelogger software. The experiments took place at the UPNM Maritime Centre's OMEY flume wave tank, equipped with a working platform, wave generator, wave absorber, and data recording devices, as shown in Fig. 4.

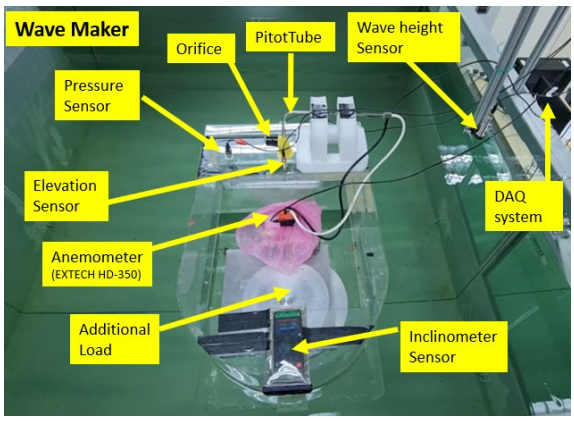

Fig. 3 *Instrumental setup in BBDB*

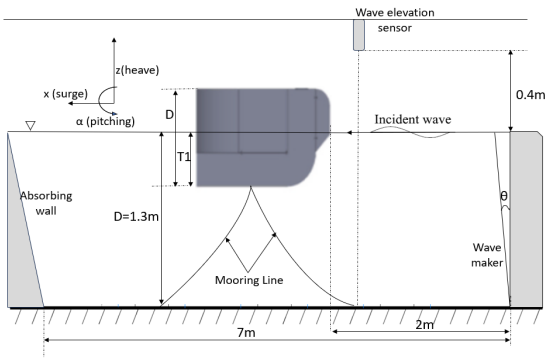

Fig. 4 *Schematic of the BBDB experiment setup*

The uncertainties of the equipment were assessed to guarantee sensitivity and calibration data compliance. The uncertainties and functions associated with the utilized instruments are in the range of 0.15 – 0.5 % in which accepted for measurement. Calibration conducted on the sensors utilized. The wave elevation sensor (KEYENCE FW-H07) had calibrated with the incoming waves generated by the flume wave maker to ensure the equality on wave height (H) and required periods. If the wave elevation sensor data do not align with the output from the wave generated, necessary adjustments can be made by modifying the voltage value, ±5V, in KEYENCE Wavelogger software.

After the calibration conducted, the error generated on all sensors confirmed to be small which less than 1%. Therefore, the wave generated had calibrated and in good agreement with the sensitivity of the wave sensor. Thus, the BBDB can proceed to the next stage of research in which to study influence of various of drafts and position of COG. To remain the LCG, the additional load will be place at the same location of LCG and TCG with 0⁰ trim and heel. The draft of BBDB can be controlled according to Archimedes principal with equation follows:

$$F_B = W = \rho g \nabla = \rho g A T \quad (1)$$

F_B is buoyancy forces (N) exerting on BBDB that has same weight of water displaced at ρ, certain density (kgm^{-3}), g, gravity acceleration (ms^{-2}), and ∇ (m^3), submerged volume. A is a submerged area while T is the draft that we control. It's worth noted that the actual draft for submerged body is measured at the bouy keel not from bottom ducting of BBDB. The dimension of ducting is as shown in Fig. 5.

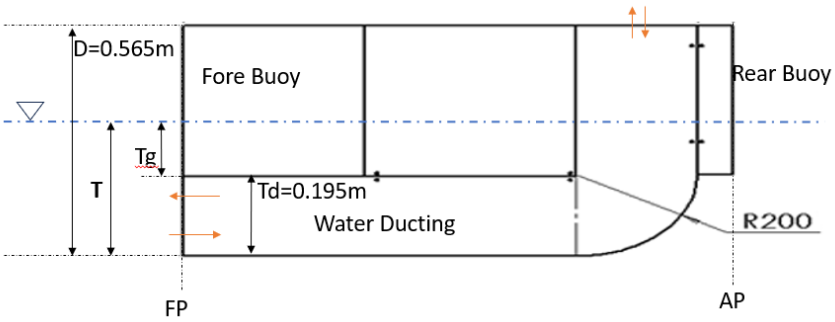

Fig. 5 *Schematic of drafts variable of BBDB (Side view)*

As shown in Fig. 5, the draft, T should be designed more than the ducting size, T_d (0.195m) so that the bidirectional water can get through into the ducting provide sufficient volume to compressed the air inside the chamber efficiently. Besides,if the draft is similar to ducting size lead to instability as well as insufficient volume of water get trhough to the ducting that reduce the performance. While for gap draft, Tg can be translated as the length between T and T_d that is significance on computing the buoyancy force and water displacement. Thus in this research, the relative draft of T/D > 0.5 utilized in this research to get best performance and have good stability as stated in [25]. It also supported by other studies made by [2] and [3] that used T/D = 0.62 throughout their research as constant. The drafts (T=0.3m, 0.33m, 0.35m, 0.4m) were selected to achieve varying T/D ratios, based on stability considerations and previous research findings that identified optimal ranges for BBDB performance. The various of relative drafts parameter matrix is illustrated in Table 2.

Table 2 *The relative drafts (T/D) parameter*

T (m)	Tg	Tg/Td	(T/D)	Mass (kg)
0.3	0.105	0.538	0.53	44.85
0.33	0.135	0.692	0.58	56.94
0.35	0.155	0.794	0.62	65.37
0.4	0.205	1.051	0.71	86.5

The COG positions were controlled by adding weights to specific locations within the BBDB's fore and aft buoyancy compartments. This allowed for precise adjustment of the longitudinal, vertical, and transverse positions of the COG, ensuring accurate testing of each configuration. Thus, the COG positions study will be conducted after obtaining an optimize T/D in Table 2. The matrix of various COG positions presented in Table 3. Notably, the COG position can be controlled by adding an additional load, m1 = 2.6 kg (0.01m x 0.02m x 0.005m) and place it in the fore bouy space horizontally as shown in Fig. 6. The new COG can be defined as follows:

$$LCG_n/VCG_n/TCG_n = \frac{\sum moment}{\sum \Delta} \quad (2)$$

Fig. 6 illustrated the different positions of COG that utilized in this research. It's worth to be noted that, the cases of 1 – 3 are located at the centreline of BBDB lead to 0⁰ of heel. For case 4 represent side location of COG

Int. Journal of Integrated Engineering Vol. 17 No. 4 (2025) p. 42-54

(port/stbd) will experience heel angle. While for case 2 (aft), will experience trim angle to aft and case 3 (fore) experience trim angle to Forward Perpendicular (FP).

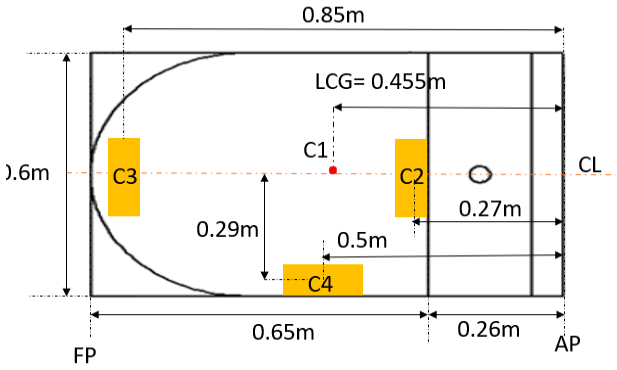

Fig. 6 *Schematic COG positions of BBDB (Top View)*

Table 3 *The COG positions matrix*

No.	Case	LCG(m)	VCG (m)	TCG (m)	Mass (kg)
C1	Exact	0.455	0.2825	0	44.85
C2	Aft	0.438	0.2781	0	47.35
C3	Fore	0.476	0.2781	0	47.35
C4	Port	0.457	0.2781	0.015	47.35

The overall methodology in this research is illustrated in Fig. 7.

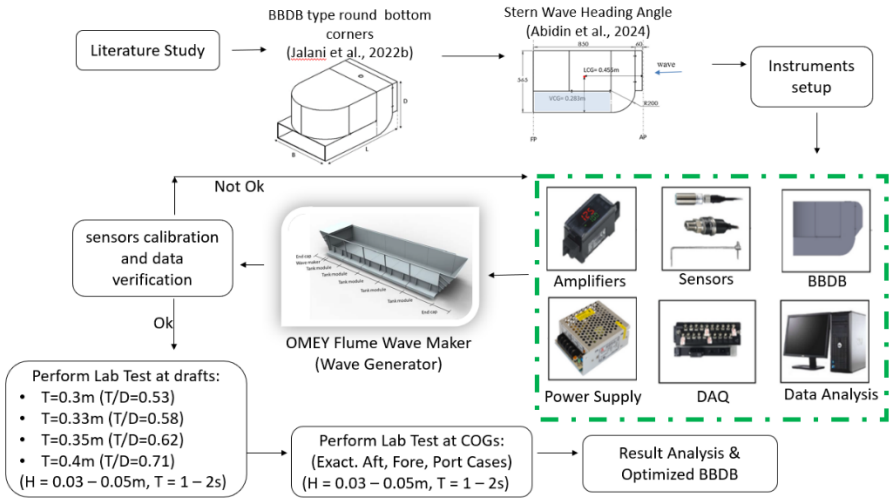

Fig. 7 *Research methodology*

Using a 2D wave tank, we evaluated the BBDB models' primary conversion efficiency in regular waves. An efficiency, pressure, and airflow graph is used to assess the performance. Hence, the primary conversion efficiency, denoted as η, is calculated by dividing the total energy of an incident wave, E_{wave}(kW) with energy airflow, E_{air}(kW) represent as the capture width ratio of with the energy. The given Eq. (3) until Eq. (7) below as Abidin et al. (2024) [20]:

$$\eta = \frac{E_{air}}{E_{wave}} \tag{3}$$

$$E_{wave} = \frac{1}{2}\rho g {A_i}^2 C_g B \quad (4)$$

$$E_{air} = \frac{1}{t}\int_0^T \Delta P(t) Q(t)\, dt \quad (5)$$

$$C_g = \frac{\omega}{2k}\left(1 + \frac{2kh}{sinh\,(2kh)}\right) \quad (6)$$

$$k = \frac{2\pi}{\lambda} \quad (7)$$

Within this framework, ρ represents the density of water (kg/m^3), A_i denotes the amplitude of an incident wave in meters (m), ω represents the angular velocity in radians per second (rad/s), h defines the water depth in meters (m), and t refers to the wave time in seconds (s). Furthermore, B represents the width of the model in meters (m), k signifies the wave number, λ denotes the wavelength measured in metres (m), C_g represents the group velocity stated in (m/s), and g represents the acceleration due to gravity (m/s^2).

According to Fig. 7, the sensor transmits air temperature, pressure, velocity, and airflow rate data to the computer employing Extech Instrument HD 350 and KEYENCE Wavelogger software. Measurements of wave heights and air pressure variations were conducted using calibrated sensors (KEYENCE FW-H07 and AP-10S), with calibration confirmed through comparison with wave generator outputs, ensuring measurement accuracy within 0.5% error margin. Exported data in Excel will be analyzed by estimating the frequent chamber pressure and airflow output via MATLAB Fast Fourier transform to calculate E_{air} as in Eq. (5). By Eq. (3), the primary conversion efficiency is identified and shown. The study examined various relative draft and COG positions at 0.03, 0.04, and 0.05 meters as in Table 2 and 3. This research was conducted across t =1.0, 1.2, 1.4, 1.6, 1.8, and 2.0 s wave periods to understand their influences. From this, a total of 144 samples were conducted to cover variables in Table 2 and 3.

3. Results and Discussion

First, an experiment was conducted to examine the variation in relative drafts. This step was necessary because the draft that yields the highest efficiency will be used in the next stage to study its impact on the center of gravity (COG) positions. Therefore, the primary conversion efficiency, as defined in Eq. (1), represents the capture width ratio of wave energy, as stated in [26] the performance of WEC at each condition given by [10]. The results for all cases are illustrated in Fig. 8 to Fig. 14. Specifically, the outcomes for various drafts (T) at a wave height (H) of 0.05m are shown in Fig. 8.

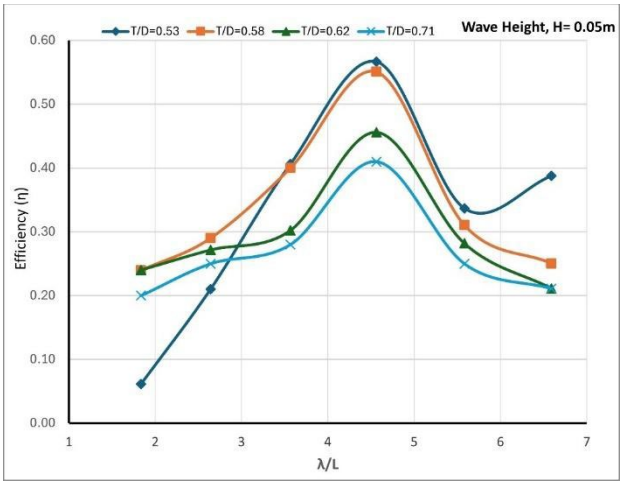

Fig. 8 *Primary conversion efficiency of relative drafts at H=0.05m*

As illustrated in Fig. 8, the BBDB exhibited its highest efficiency (η) at T = 0.3m (T/D = 0.53), achieving a value of 56.7%. This was followed by T = 0.33m (T/D = 0.58),(η = 55%), T = 0.35m (T/D = 0.62),(η = 45.8%), and T = 0.40m (T/D = 0.71) (η = 41%). Validation can be made by comparing the result of T = 0.35m (T/D = 0.62) with Ref. [24] at (η = 46.2%) and {Formatting Citation} at (η = 45.6%) of wave height (H) of 0.05m. The percentage difference between the current and prior study is presented in Table 4.

Int. Journal of Integrated Engineering Vol. 17 No. 4 (2025) p. 42-54

Table 4 *The percentage difference of η at T = 0.35m (T/D = 0.62), H=0.05*

Current (%)	Jalani et al., (2022) [19] (%)	Abidin et al., (2024) [20] (%)	Average (%)	Percentage (%)
45.8	46.2	45.6	45.9	0.22

This slight difference shows a significant concurrence and agreement between the data produced in this study and the findings from prior research. It is important to mention that some variation experienced due to the fact that [19] carried out their study in a 3D ocean tank, which simulated a longer time period (1 to 5 s) and took into account a broader range of wave heights (0.05 – 0.15 m). The results presented in [20] are nearly same because this experiment is a continuation of their previous investigation at the same wave tank.

Moreover, it is evident that for λ/L values between 3 and 5, all relative drafts demonstrate a significant and rapid rise in η, reaching its maximum in the range of λ/L = 4 to 5, and then experiencing a dramatic decline, with η decreasing to half of its maximum value. In addition, the results indicate that a T of 0.40m (T/D = 0.71) does not effectively optimise BBDB performance, since it produces the lowest η. Fig. 9 exhibits comparable patterns.

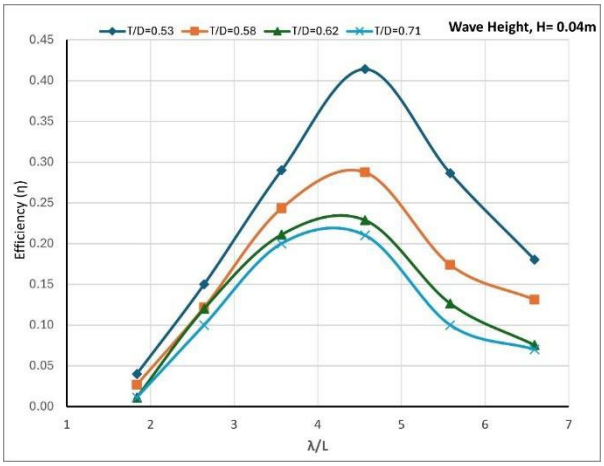

Fig. 9 *Primary conversion efficiency of relative drafts at H=0.04m*

According to Fig.9 illustrated the BBDB's relative draft of T = 0.3m (T/D = 0.53) remain at the highest η of 41%, followed by T = 0.33m (T/D = 0.58),(η = 29%), T = 0.35m (T/D = 0.62),(η = 22.8%), and T = 0.40m (T/D = 0.71) (η = 21%). Similar to Fig. 8, at λ/L = 3 to 5, the efficiency increased rapidly before it started to reduce dramatically, which is half the efficiency of the peak. It can be observed, loss of performance 50% when BBDB operate in draft more than 62% of BBDB depths.

In Fig. 10, examining H=0.03m demonstrates that the relative draft of T = 0.3m (T/D = 0.53) yielded the maximum efficiency (η =28%). This was followed by T = 0.33m (T/D = 0.58),(η = 24%), T = 0.35m (T/D = 0.62),(η = 16.7%), and T = 0.40m (T/D = 0.71) (η = 16.5%). The observed results indicate a consistent trend with H=0.05m and 0.04m, where the draft more than 60% of BBDB does not contribute to the optimization of BBDB, resulting in the lowest efficiency.

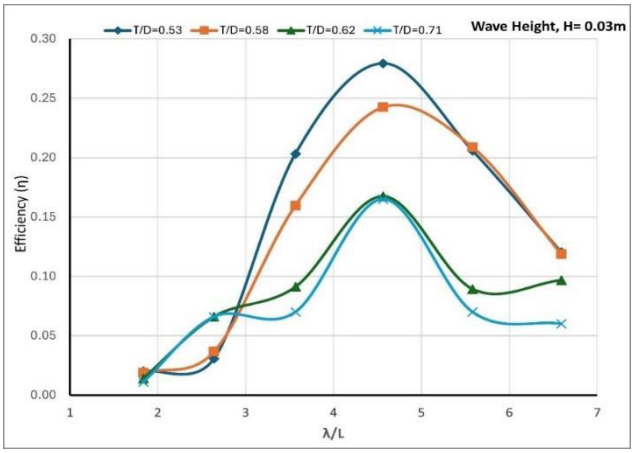

Fig. 10 *Primary conversion efficiency of relative drafts at H=0.03m*

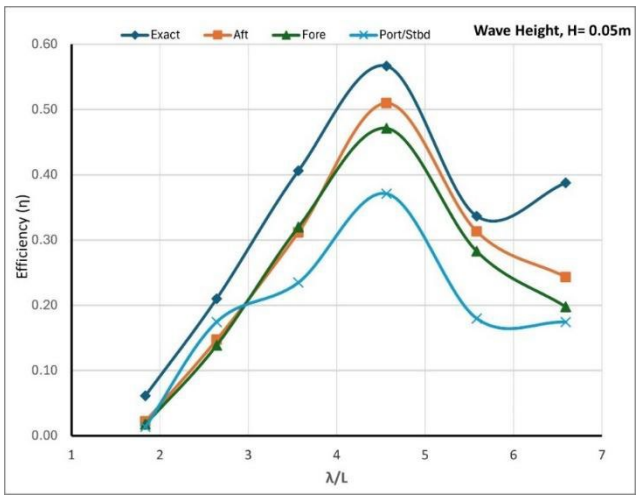

Fig. 11 *Primary conversion efficiency of COG positions at H=0.05m*

As illustrated in Fig. 11, the BBDB exhibited its highest efficiency (η) at Exact COG (0.455, 0, 0.2825), achieving a value of 56.7%. This was followed by Aft COG (0.438, 0, 0.2781),(η = 50.9%), Fore COG (0.476, 0, 0.2781),(η = 47.1%), and Port COG (0.457, 0.015, 0.2781),(η = 37.1%). It can observed that, the similar trend appear for λ/L values between 3 and 5, all COG positions demonstrate a significant and rapid rise in η, reaching its maximum in the range of λ/L = 4 to 5, and then experiencing a dramatic decline, with η decreasing rapidly. We can see that, the Port COG at heeling angle does not effectively optimise BBDB performance, since it produces the lowest η. Fig. 12 exhibits similar patterns.

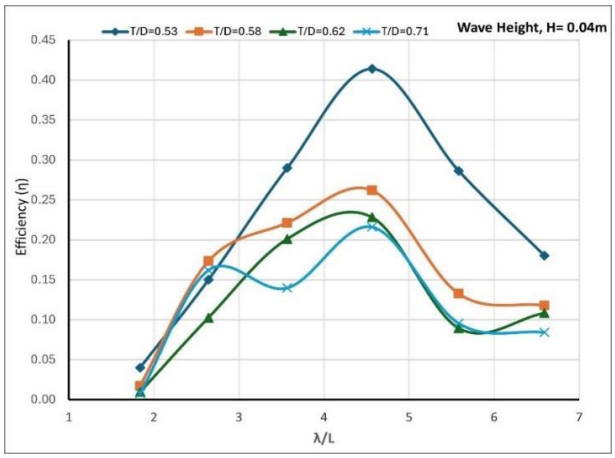

Fig. 13 *Primary conversion efficiency of COG positions at H=0.03m*

In Fig. 13 illustrated the highest efficiency (η) at Exact COG (0.455, 0, 0.2825), achieving a value of 28%. This was followed by Aft COG (0.438, 0, 0.2781),(η = 19.9%), Fore COG (0.476, 0, 0.2781),(η = 18.1%), and Port COG (0.457, 0.015, 0.2781),(η = 16.1%). It can observed that, the similar trend appear for λ/L values between 3 and 5, and in the range of λ/L = 4 to 5 except for Fore COG that shows the highest at λ/L= 3 to 4, before experiencing η a dramatic decline. Indeed, the Port COG unable to harness substantial wave energy effectively, resulting in suboptimal airflow rates and differential pressures. This limitation is primarily attributed to the repetitive pitch and heave motion exhibited by the BBDB.

Fig. 8 to Fig. 10 indicate that the findings exhibit similar hydrodynamic characteristics to those explained by Tupper and Birk for ships [22, 24]. It can be concluded that the BBDB with a lower relative draft (T/D) experiences greater heave and pitching motions because it is less submerged, leading to a higher center of buoyancy (COB) relative to its center of gravity (COG). This makes the BBDB more responsive to the moments created by waves, thereby being more affected by surface wave dynamics. However, while increased heave and pitching can be desirable for certain dynamic applications, they often come at the cost of reduced stability. Ships with a lower T/D can be less stable in heavy seas.

Fig. 11 to Fig. 13 illustrate the variation of COG positions in relation to performance. It can be observed that Case 1 has a higher Vertical Center of Gravity (VCG) compared to the others due to the additional load being placed in the fore buoyancy, which is lower than the exact COG. Thus, in line with prior studies, it can be observed that as VCG increases, the pitching motion also increases. When the VCG is higher, the ship has a higher moment arm relative to the COB, leading to larger pitching angles and more pronounced up-and-down movements at the aft perpendicular (AP) and forward perpendicular (FP). As a result, Case 1 (Exact COG) presents the highest efficiency obtained. In contrast, other cases with a lower VCG reduce pitching motion. With a lower VCG, the BBDB is more stable and has less tendency to pitch because the moments around the COB are smaller. Additionally, for Case 4 (Port COG), where the BBDB is at a heeling angle, the motion constraints act as damping for the pitching and heaving motions, resulting in reduced movement. Consequently, this impediment results in less pneumatic energy being captured in the air chamber from the wave energy, with a significant portion of the remaining energy dissipating as heat and vortices. These findings are in line with those of Tupper, Birk, John Ashlin et al., Wu et al., Jalani et al., and Abidin et al. [17-18, 20-22, 24]. The identification of optimal draft and COG positions can directly inform the design of next-generation BBDBs, ensuring higher efficiency in energy conversion. These insights can be applied during the initial design phase to select appropriate geometrical configurations. Adjustments to COG positions allow for fine-tuning of BBDBs to match site-specific wave conditions, making these devices more adaptable for use in diverse marine environments, from coastal to offshore applications. The reduction in drag through optimized draft selection contributes to improved stability and lower maintenance requirements, which is crucial for reducing operational costs in commercial-scale WEC deployments.

4. Conclusion

This study aimed to examine the characteristics and effectiveness of the BBDB with different relative drafts and COG positions. Regular waves were employed in a 2D Flume wave tank to test the models. The following concise summary of the study's findings is provided:

- The research was validated against prior studies conducted by Jalani et al. (2022) and Abidin et al. (2024) at H=0.05m, with a percentage difference of only 0.22%, as shown in Table 4. This validation demonstrates the reliability and consistency of the experimental results.
- The BBDB's relative draft of T = 0.3m (T/D = 0.53) with an Exact COG configuration achieved the highest efficiency across all wave heights tested. Conversely, the draft of T = 0.4m (T/D = 0.71) with Port/Stbd COG positions was found to have the lowest efficiency, highlighting the importance of optimal draft and COG positioning for performance enhancement.

In addition, this study also provides practical insights for the design and operation of WEC where specific dynamic responses like high heave and pitch are desired. Balancing these dynamics with stability and safety is crucial. Engineering solutions, such as active stabilizers or specific hull designs, can help manage these motions effectively. Maintaining an appropriate center of gravity is essential for stability; an excessively high center of gravity can cause dangerous instability, especially in rough seas [22]. This study highlights the balance between achieving high heave and pitching (low T/D and high VCG) and ensuring stable motion (high T/D and low VCG) to optimize BBDB performance and safety.

Thus, we conclude that a draft of T/D = 0.53 with an Exact COG (upright position) allows sufficient water to pass through the ducting, leading to effective compression in the air chamber and improved BBDB performance while maintaining stability. This finding is crucial for future BBDB designs aiming for higher efficiency and operational effectiveness. As proposed by Abidin et al. (2024), the Froude scaling technique will be employed to extrapolate power to a 1:13 scale for future studies, ensuring the applicability of the results to full-scale wave energy converters. Additionally, a risk assessment of the wave energy converter (WEC), as proposed by Abdullah

et al. (2021), will be conducted for the prototype BBDB once its power generation capabilities are determined [27].

Acknowledgement

The authors gratefully acknowledge the financial support provided by Akaun Amanah Industri Bekalan Elektrik (AAIBE) under the grant number UPNM/2018/AAIBE-KETTHA/TK/1/P4 and the Fundamental Research Grant Scheme (FRGS) under the grant number FRGS/1/2020/TK0/UPNM/02/3, which made the successful execution of this project possible.

The successful execution of this project was achieved through the financial support provided by Akaun Amanah Industri Bekalan Elektrik (AAIBE) under the grant number UPNM/2018/AAIBE-KETTHA/TK/1/P4 and FRGS/1/2020/TK0/UPNM/02/3.

Conflict of Interest

Authors declare that there is no conflict of interests regarding the publication of the paper.

Author Contribution

The authors confirm contribution to the paper as follows: ***study conception and design:*** *Noh Zainal Abidin, Mohd Rashdan Saad, Mohd Rosdzimin Abdul Rahman;* ***data collection:*** *Noh Zainal Abidin, Mohd Norsyarizad Razali, Mohamad Azrin Abd Azis;* ***analysis and interpretation of results:*** *Noh Zainal Abidin, Ameer Suhel;* ***draft manuscript preparation:*** *Noh Zainal Abidin Mohd Najib Abdul Ghani Yolhamid, Zulkifly Mat Radzi. All authors reviewed the results and approved the final version of the manuscript.*

References

[1] Gunn, K., & Stock-Williams, C. (2012). Quantifying the global wave power resource. *Renewable energy*, *44*, 296-304. https://doi.org/10.1016/j.renene.2012.01.101

[2] Tan, W. C., Chan, K. W., & Ooi, H. (2017, July). Study of the potential of wave energy in Malaysia. In *AIP Conference Proceedings* (Vol. 1865, No. 1). AIP Publishing.

[3] Amarasekara, H. W. K. M., Abeynayake, P. A. G. S., Fernando, M. A. R. M., Atputharajah, A., Uyanwaththa, D. M. A. R., Gunawardane, S. D. G. S. P., Gerdin, L., Keijser, M. R., Fahraeus, M. W., Fernando, I. M. K., & Cooray, V. (2014). A prefeasibility study on ocean wave power generation for the southern coast of Sri Lanka: Electrical feasibility. *Int. J. Distrib. Energy Resour. Smart Grids*, *10*(2), 79-93.

[4] Suhel, A., Abdul Rahim, N., Abdul Rahman, M. R., Bin Ahmad, K. A., Teoh, Y. H., & Zainal Abidin, N. (2021). An experimental investigation on the effect of ferrous ferric oxide nano-additive and chicken fat methyl ester on performance and emission characteristics of compression ignition engine. *Symmetry*, *13*(2), 265. https://doi.org/10.3390/sym13020265

[5] Babarit, A. (2017). *Ocean wave energy conversion: resource, technologies and performance*. Elsevier. https://doi.org/10.1016/C2016-0-01219-6

[6] Sheng, W. (2019). Wave energy conversion and hydrodynamics modelling technologies: A review. *Renewable and Sustainable Energy Reviews*, *109*, 482-498. https://doi.org/10.1016/j.rser.2019.04.030

[7] Jebli, M., & Chagdali, M. (2018, April). Hydrodynamic characteristics of an OWC device for Wave Energy Conversion. In *2018 Renewable Energies, Power Systems & Green Inclusive Economy (REPS-GIE)* (pp. 1-5). IEEE. https://doi.org/10.1109/REPSGIE.2018.8488849

[8] Falcão, A. F., & Henriques, J. C. (2016). Oscillating-water-column wave energy converters and air turbines: A review. *Renewable energy*, *85*, 1391-1424. https://doi.org/10.1016/j.renene.2015.07.086

[9] Babarit, A., Hals, J., Muliawan, M. J., Kurniawan, A., Moan, T., & Krokstad, J. (2012). Numerical benchmarking study of a selection of wave energy converters. *Renewable energy*, *41*, 44-63. https://doi.org/10.1016/j.renene.2011.10.002

[10] Zhang, D., Li, W., & Lin, Y. (2009). Wave energy in China: Current status and perspectives. *Renewable energy*, *34*(10), 2089-2092. https://doi.org/10.1016/j.renene.2009.03.014

[11] Badhurshah, R., Samad, A., & Karthikeyan, T. (2014, February). Oscillating water column wave energy system—A prospective. In *2014 First International Conference on Automation, Control, Energy and Systems (ACES)* (pp. 1-5). IEEE.

[12] Imai, Y., Nagata, S., Toyota, K., & Murakami, T. (2014). An experimental study on primary efficiency of a wave energy converter" backward bent duct buoy" in regular wave conditions. *Journal of the Japan Society of Naval Architects and Ocean Engineers*, *19*. https://doi.org/10.2534/jjasnaoe.19.79

[13] Falcão, A. F., & Henriques, J. C. (2014). Model-prototype similarity of oscillating-water-column wave energy converters. *International Journal of Marine Energy*, *6*, 18-34. https://doi.org/10.1016/j.ijome.2014.05.002

[14] Abidin, N. Z., Leblond, C., Yolhamid, M. N. A. G., Zarim, M. A. U. A. A., Ibrahim, F., & Suhel, A. (2021). Investigation of numerical hydrodynamic performance of deformable hydrofoil (Applied on blade propeller). *Transactions on Maritime Science*, *10*(02), 414-438. https://doi.org/10.7225/toms.v10.n02.012

[15] Toyota, K., Nagata, S., Imai, Y., & Setoguchi, T. (2009, September). Research for evaluating performance of OWC-type wave energy converter 'Backward Bent Duct Buoy'. In *Proceedings of the 8th European Wave and Tidal Energy Conference* (pp. 901-913).

[16] Ashlin, S. J., Sundar, V., & Sannasiraj, S. A. (2016). Effects of bottom profile of an oscillating water column device on its hydrodynamic characteristics. *Renewable Energy*, *96*, 341-353. https://doi.org/10.1016/j.renene.2016.04.091

[17] Wu, M., Stratigaki, V., Troch, P., Altomare, C., Verbrugghe, T., Crespo, A., Cappietti, L., Hall, M., & Gómez-Gesteira, M. (2019). Experimental Study of a Moored Floating Oscillating Water Column Wave-Energy Converter and of a Moored Cubic Box. *Energies*, *12*(10), 1834. https://doi.org/10.3390/en12101834

[18] Gadelho, J. F. M., Rezanejad, K., Xu, S., Hinostroza, M., & Soares, C. G. (2021). Experimental study on the motions of a dual chamber floating oscillating water column device. *Renewable Energy*, *170*, 1257-1274.

[19] Jalani, M. A., Ismail, N. I., Saad, M. R., Samion, M. K. H., Imai, Y., Nagata, S., & Rahman, M. R. A. (2022). Experimental study on a bottom corner of the floating WEC. *Ocean engineering*, *243*, 110237. https://doi.org/10.1016/j.oceaneng.2021.110237

[20] Abidin, N.Z., Rosdzimin, M., Rahman, A., Razali, M.N., Suhel, A., Jalani, M.A., Ibrahim, F., Najib, M., Yolhamid, A.G., Azrin, M., & Azis, A. (2024) Experimental study on heading angle effects for optimized wave energy converter (WEC) type backward bent duct buoy (BBDB). *Journal of Engineering Science and Technology, 19(2),* 98-113.

[21] TTupper, E. C. (2013). *Introduction to naval architecture*. Butterworth-Heinemann.

[22] Ibrahim, F., Razali, M. N., & Abidin, N. Z. (2021). Content analysis of international standards for human factors in ship design and operation. *Transactions on Maritime Science*, *10*(02), 448-465. https://doi.org/10.7225/toms.v10.n02.014

[23] Birk, L. (2019). Fundamentals of ship hydrodynamics: Fluid mechanics, ship resistance and propulsion. John Wiley & Sons.

[24] Jalani, M. A., Ismail, N. I., Saad, M. R., Samion, M. K. H., Imai, Y., Nagata, S., & Rahman, M. R. A. (2022). Experimental study on a bottom corner of the floating WEC. *Ocean engineering*, *243*, 110237. https://doi.org/10.1016/j.oceaneng.2021.110237

[25] Alamian, R., Shafaghat, R., Bayani, R., & Amouei, A. H. (2017). An experimental evaluation of the effects of sea depth, wave energy converter's draft and position of centre of gravity on the performance of a point absorber wave energy converter. *Journal of Marine Engineering & Technology*, *16*(2), 70-83. https://doi.org/10.1080/20464177.2017.1282718

[26] Elhanafi, A., Macfarlane, G., & Ning, D. (2018). Hydrodynamic performance of single–chamber and dual–chamber offshore–stationary Oscillating Water Column devices using CFD. *Applied Energy*, *228*, 82-96. https://doi.org/10.1016/j.apenergy.2018.06.069

[27] Abdullah, M. A., Abidin, N. Z., Radzi, Z. M., Ahmad, M. A., Munikanan, V., Razali, M. N., & Ismail, N. (2021). Risk assessment of wave energy converter at Kuantan Port, Pahang. *Transactions on Maritime Science*, *10*(02), 318-329. https://doi.org/10.7225/toms.v10.n02.002